Bulletin of Engineering Geology and the Environment (2020) 79:3483–3496
https://doi.org/10.1007/s10064-020-01780-4

ORIGINAL PAPER

A simplified method to analyze the load on composite retaining structures based on a novel soil arch model

Xiaoyan Zhao[1] · Kunpeng Li[1] · Dian Xiao[1]

Received: 3 June 2019 / Accepted: 20 March 2020 / Published online: 3 April 2020

Abstract

Soil arch effect has been widely used in the determination of pile spacing, whereas its application on the design of composite retaining structures to stabilize potentially unstable slopes is still rare. As a typical composite retaining structure, stabilizing piles combined retaining wall could effectively avoid slope failure, while the problem of evaluating the load distribution between stabilizing piles and retaining wall based on soil arch effect remains to be solved. In this paper, a novel soil arch model is proposed and used aiming to theoretically analyze the soil arch effect on the load against stabilizing piles and retaining wall. The results show that the load acting on stabilizing piles should be the residual sliding force derived from rear soil mass, and the load against retaining wall should be the maximum value between the Coulomb's active earth pressure derived from sliding wedge before soil arch and the residual sliding force produced by front soil mass. Then, on this basis, a simplified method for calculating the load on stabilizing piles and retaining wall respectively considering the soil arch effect is put forward. A railway cutting slope reinforced with stabilizing piles combined with retaining wall is taken as an application case, and the simplified method is adopted to quantitatively analyze the soil arch effect on the load distribution between stabilizing piles and retaining wall. The conclusion of this paper would provide useful help toward the process of safer and more economical design of composite retaining structures in slope engineering harness.

Keywords Simplified method · Soil arch model · Composite structure · Stabilizing pile · Retaining wall · Load distribution

Introduction

With the rapid development of infrastructure construction in mountainous regions, excavation of cutting slope has become a crucial cause for excessive slope movement and slope failure (Ehrlich and Silva 2015; Ersöz and Topal 2018; Hu and Ma 2018; Mohammadi and Taiebat 2016). Currently, it is widely accepted that stabilizing pile is an effective measure to ensure the stability of cutting slope (Galli and di Prisco 2013; Li et al. 2019; Lirer 2012; Qin et al. 2017; Xiao et al. 2017; Zhang et al. 2018). Claystone is known worldwide as a problematic rock mass with poor engineering properties, triggering many geological hazards (Alejano et al. 2010; Aydin et al. 2004; Rincon et al. 2016; Yilmazer et al. 2003; Zhang et al. 2017). Especially in southwest China, claystone slope reinforced with stabilizing piles frequently suffers from large movements and slope failures between the piles due to its high weathering and disintegration potential. In order to prevent such engineering hazards, geotechnical engineers must reconsider corresponding issues related to the mechanism of slope failure and redesign the reinforcement measures.

Several advanced techniques that have been used to deal with such problems are stabilizing piles combined with retaining wall, sheet pile wall or soil nail wall (Railway Design Code of retaining structures of railway embankment (Standardization Administration of China 2006)), seen in Fig. 1. Among these techniques, stabilizing piles combined with retaining wall is the most widely used one in engineering practice due to that such structure is easy to construct. Unfortunately, although such a structure is designed and used extensively, the problem of evaluating the load distribution between stabilizing piles and retaining wall still remains to be studied.

The conventional methods for the design of stabilizing piles combined with retaining wall are mainly based on the

✉ Xiaoyan Zhao
xyzhao2@swjtu.cn

[1] Department of Geology Engineering, Faculty of Geosciences and Environmental Engineering, Southwest Jiaotong University, 999 Xi'an Road Pi County, Chengdu 611756, Sichuan, China

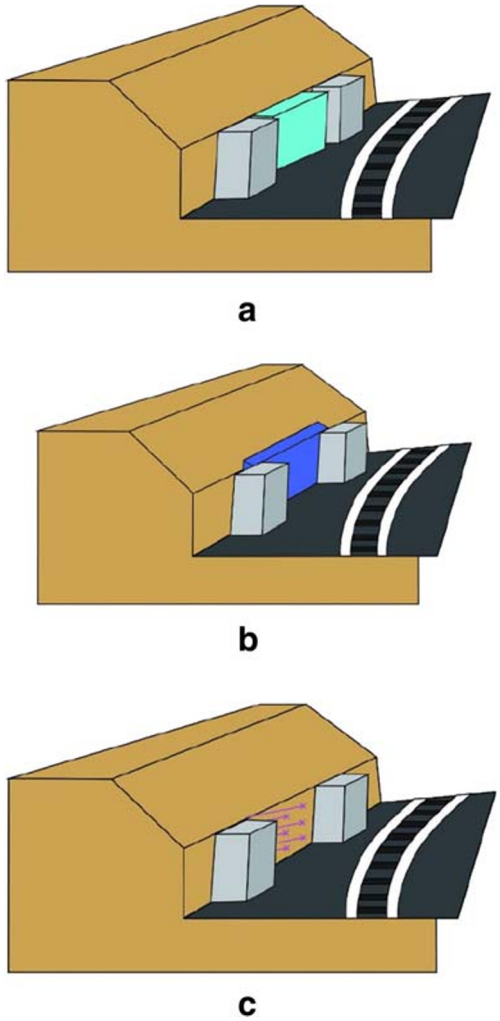

Fig. 1 Composite retaining structures. **a** Stabilizing piles with retaining wall. **b** Stabilizing piles with cantilever wall. **c** Stabilizing piles with soil nail wall

design theory of individual pile or wall structure with limit equilibrium theory (Ito and Matsui 1975; Krabbenhoft 2019; Martin et al. 2019; Pain et al. 2017; Vrecl Kojc and Trauner 2010; Zhou et al. 2018). For the load on stabilizing piles, it adopts the residual sliding force calculated with the transfer coefficient method (Bi et al. 2012; Zheng et al. 2015). For the load against retaining wall, it is always obtained by three methods: (1) active earth pressure estimated based on Coulomb theory is used as the load on retaining wall (Standardization Administration of China 2006)); (2) increase soil strength parameters, then adopt the same method as (1); (3) Active earth pressure estimated based on Coulomb theory multiplied by a reduction coefficient (0.7 or 0.8) is used as the load on retaining wall (Standardization Administration of China 2006). However, such methods all have ignored or unreasonably considered the soil arch effect, potentially leading to inappropriate design of stabilizing piles and retaining wall, as well as overinvestment.

Considering the soil arch effect reasonably is of great significance for designing composite retaining structures better. Over last few decades, various studies on soil arch effect have been carried out by many researchers (Ahmadi and Seyedi Hosseininia 2018; Chen and Martin 2002; Chevalier et al. 2007; Handy 1985; Iglesia et al. 2014; Khatami et al. 2019; McKelvey III 1994; Terzaghi 1943; Vardoulakis et al. 1981). Although such studies have provided many conveniences to the design of stabilizing piles, most of them mainly involves the determination of pile spacing (Lai et al. 2018; Li et al. 2015; Pirone and Urciuoli 2018; Wu et al. 2017), and contributions on the design of composite structures such as stabilizing piles combined with retaining wall are still rare. Jiang et al. (Jiang et al. 2010), through measuring earth pressure in the field test, briefly described the load distribution characteristics of earth pressure against composite retaining structures considering the soil arch effect. Liang et al. (Liang et al. 2014) analyzed the influence of soil arch shape on the load distribution against composite retaining structures by physical model test. Unfortunately, such limited studies are only concerned with qualitative analysis of soil arch effect on the load distribution rather than quantitative analysis and cannot be used directly in the design of composite retaining structures.

In this paper, a novel soil arch model was proposed, based on the Local Standard of Code in Chongqing City for the design of geological hazard prevention engineering (Urban And Rural Construction Committee, 2004). Then, the influence of soil arch on the load against composite retaining structures was theoretically analyzed, and a simplified method for calculating the load on stabilizing piles and retaining wall was put forward. Taking a cutting slope located in Bazhong-Dazhou Railway as an example, when the soil arch effect was considered or not, the load distribution between stabilizing piles and retaining wall was quantitatively evaluated and compared. Consequently, a better design of stabilizing piles and retaining wall was obtained. This paper favorably paves the way for potential application of soil arch on the optimized design of composite retaining structures.

Theoretical background

Novel soil arch model

In order to analyze soil arch effect better, researchers have raised plenty of assumptions on the shape of soil arch, including catenary (Handy 1985; Kingsley 1989), circular (Harrop-williams 1987), parabola (Goel and Patra 2008), and many other shapes. Although researchers could find abundant proof for their hypotheses, such hypotheses are unsuitable for engineering practice due to that they are overly complex to use.

In the Local Standard of Code in Chongqing City for the design of geological hazard prevention engineering

(Standardization Administration of Chongqing, China 2004), the shape of soil arch is supposed to be an isosceles right triangle, and the inclination angle α, which is the angle between the back of pile and the soil arch, equals 45°, as seen in Fig. 2a. On this basis, an assumption that the height of soil arch is constant along the vertical direction is put forward, as shown in Fig. 2b. Consequently, a novel 3D model is obtained to denote the characteristics of soil arch (seen in Fig. 3).

From Fig. 2a, the pile Z_1 and Z_2 form a soil arch mass $B_1BB_2O_2A_2AA_1O_1B_1$ between them, where B_1BB_2 and A_1AA_2, being both isosceles right triangles, are the outer and inner edges of soil arch, respectively. The line O_1OO_2 is the axis of the soil arch. Therefore, the height of soil arch axis (h), the height of the inner edge of soil arch mass (h_1), and the height of the outer edge of soil arch mass (h_2) can be expressed as

$$h = \frac{(a+d)}{2} \tag{1}$$

$$h_1 = \frac{d}{2} \tag{2}$$

$$h_2 = a + \frac{d}{2} \tag{3}$$

where a is the width of pile, and d denotes the clear distance between piles.

Hypotheses on the characteristics of soil arch

Deformation or failure of soil arch does not occur

In order to analyze the soil arch effect on the load against stabilizing piles and retaining wall, the soil arch should persist with integrity. Thus, a hypothesis that the deformation or failure of soil arch does not occur is put forward. Considering that soil arch is more compact than surrounding soil mass, its mechanical properties should be significantly better than the surrounding soil. In light of the hypothesis that the deformation or failure of soil arch does not occur, thus the force acting on soil arch is less than the shear strength of the arch. Consequently, the arch is in elastic state and could be considered to be rigid compared with the surrounding soil.

In actual construction, since stabilizing piles are built first, followed by slope cut, and then retaining wall built between in the piles, the soil arch could have time to form. The arch separates retained soil into three parts: soil arch mass, front soil mass, and rear soil mass, as shown in Fig. 2b. Due to the effect of soil arch, the residual sliding force derived from rear soil mass is passed to the stabilizing piles only, rather than the stabilizing piles and retaining wall together. As for the load on the retaining wall, it just originates from front soil mass, since the arch cuts the ties between such wall and rear soil mass.

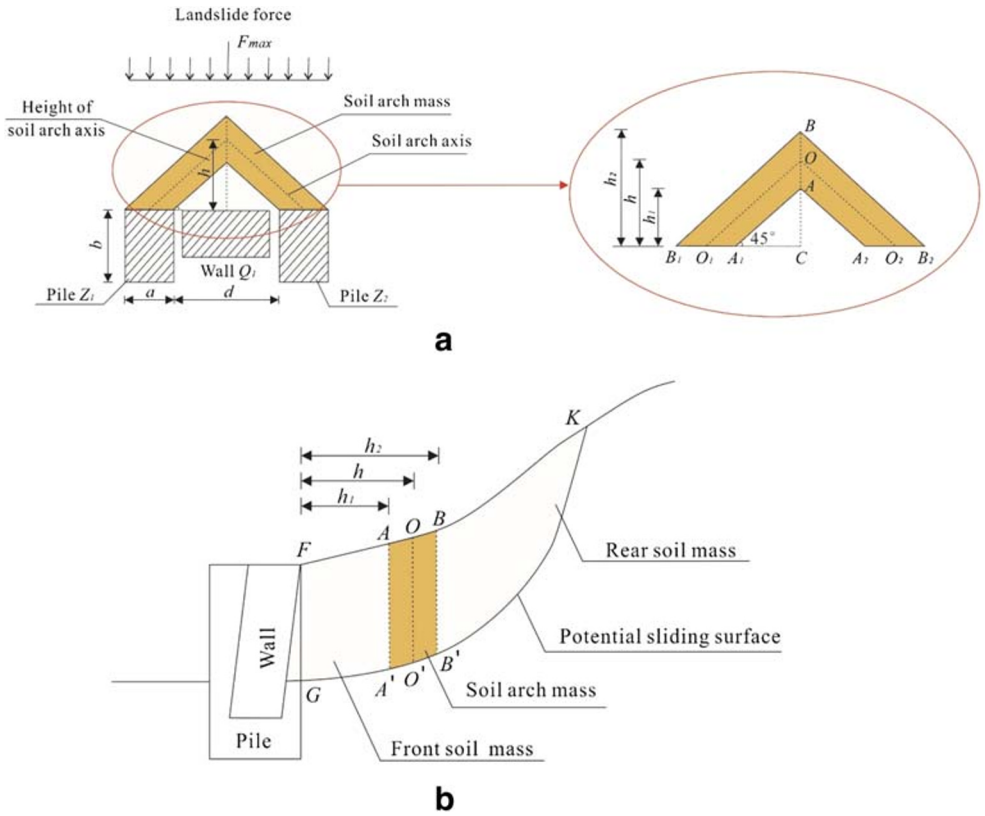

Fig. 2 Cross section of soil arch. **a** Top view. **b** Side view

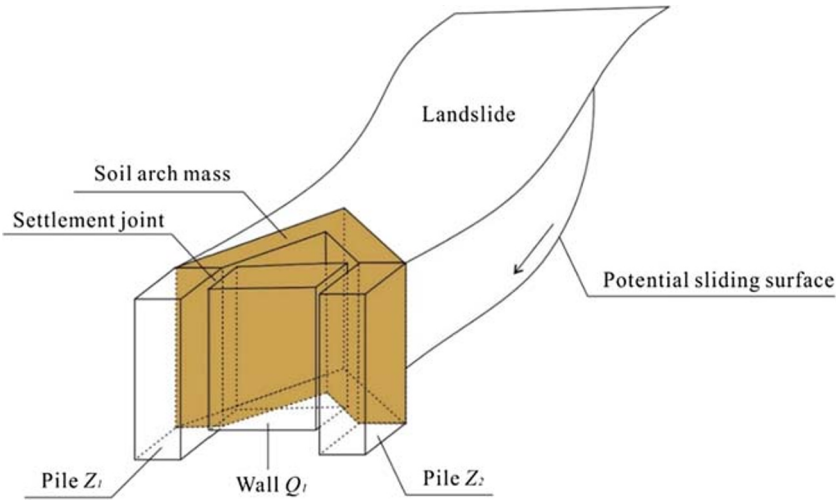

Fig. 3 Novel 3D model of soil arch

The height of soil arch axis is adopted as the height of soil arch

As shown in Fig. 2a, if pile width a is 2 m, then arch thickness will be approximately 1.4 m. Since the arch thickness is much smaller than the length of retained soil mass, the height of soil arch axis is adopted as the height of soil arch for a simplified analysis. Under such a hypothesis, the scope of front and rear soil mass changes from AFGA', KBB' into OFGO', KOO', respectively, as shown in Fig. 2b. Thus, the design load against stabilizing piles and retaining wall is increased, which would result in a safer design.

Simplified method for calculating the load on composite retaining structures

Load on stabilizing piles

Due to the existence of soil arch, the load on stabilizing piles should be the residual sliding force derived from rear soil mass KOO', rather than the retained soil KFG, as shown in Fig. 2b. In this paper, the transfer coefficient method proposed by most design codes is adopted to calculate the residual sliding force.

Besides, a settlement joint between the retaining wall and the adjacent piles is set (see Fig. 3) and filled with a mixed material of hemp rope and asphalt, which is mainly for preventing the soil between pile and wall from slipping out after heavy rainfall. Such mixed material is a kind of flexible material, thus the load against stabilizing piles and retaining wall is independent and will not affect each other.

Load on retaining wall

As mentioned before, the load against retaining wall just originates from the front soil mass and cannot be affected by the soil mass after the arch, thus it adopts the active earth pressure or residual sliding force derived from front soil mass. Such two forces are obtained by the limit equilibrium method and transfer coefficient method, respectively.

According to the different locations of soil arching axis (see Fig. 4), the analysis can be divided into two cases:

1. The soil arching axis OO' is located behind the top of failure surface BH, as shown in Fig. 4a. In this case, the range of sliding wedge and front soil mass is HFB and OFIO'. Then the active earth pressure produced by the wedge HFB is denoted by P_{1FB}, and the residual sliding force derived from front soil mass OFIO' is represented by E_{1FI}. Consequently, the load against retaining wall F equals the maximum between P_{1FB} and E_{1FI}, $F = \max(P_{1FB}, E_{1FI})$;
2. The soil arching axis OO' is located before the top of failure surface BH, as seen in Fig. 4b. In this case, the range of front soil mass is still OFIO', whereas the range of sliding wedge changes into OFBE. Thus, P_{2FB} and E_{2FI} are adopted to denote the active earth pressure produced by the wedge OFBE and the residual sliding force resulted from front soil mass OFIO'. Consequently, the load against retaining wall F equals the maximum between P_{2FB} and E_{2FI}, $F = \max(P_{2FB}, E_{2FI})$.

The soil arch axis located behind the top of the active failure surface

When the soil arching axis is located behind the top of the failure surface, the residual sliding force E_{1FI} derived from the soil mass OFIO' could be calculated based on the transfer coefficient method.

In order to solve the active earth pressure P_{1FB} produced by the wedge HFB, the force analysis of such wedge should be carried out first, as shown in Fig. 5.

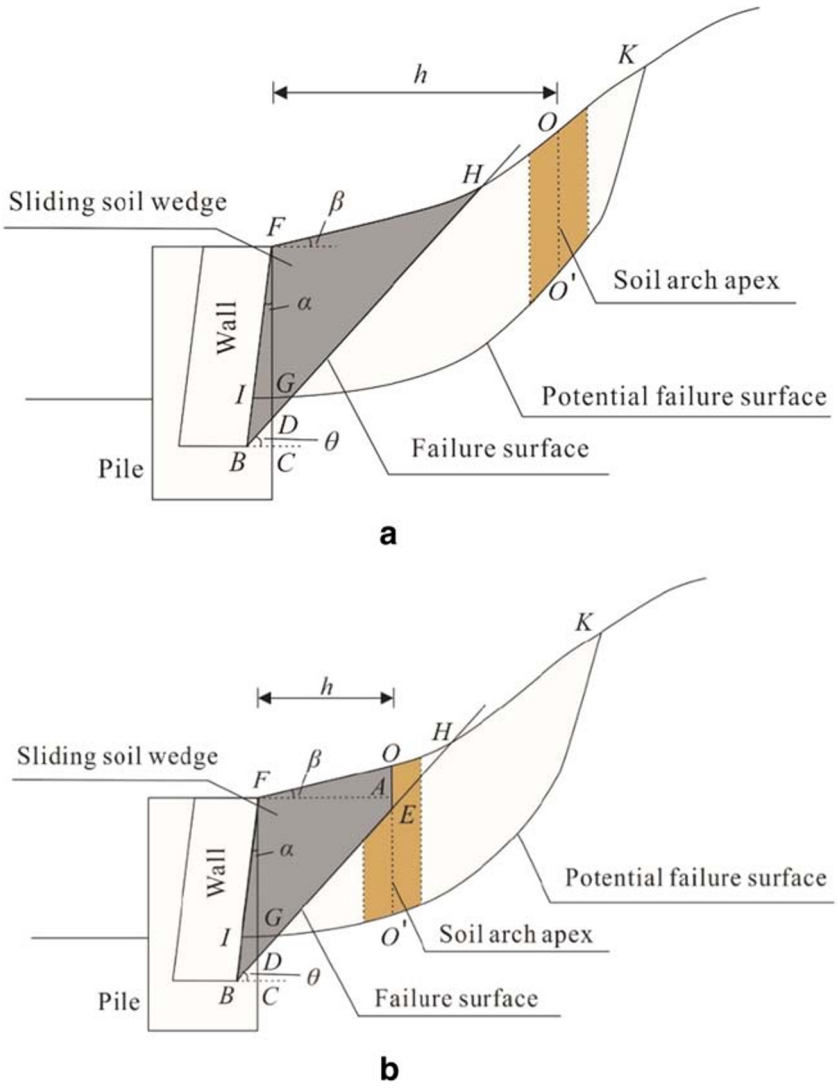

Fig. 4 Calculation model of the load on retaining wall. **a** Soil arching axis is located behind the top of failure surfac. **b** Soil arching axis is located before the top of failure surface

Where, W is the weight of soil wedge; R is the reaction force acting on the active failure surface; δ, φ, and θ are the friction angle between the back of retaining wall and the retained soil, the friction angle of the retained soil, and the angle between the active failure surface and the horizontal, respectively; α and β are the angle between the back of

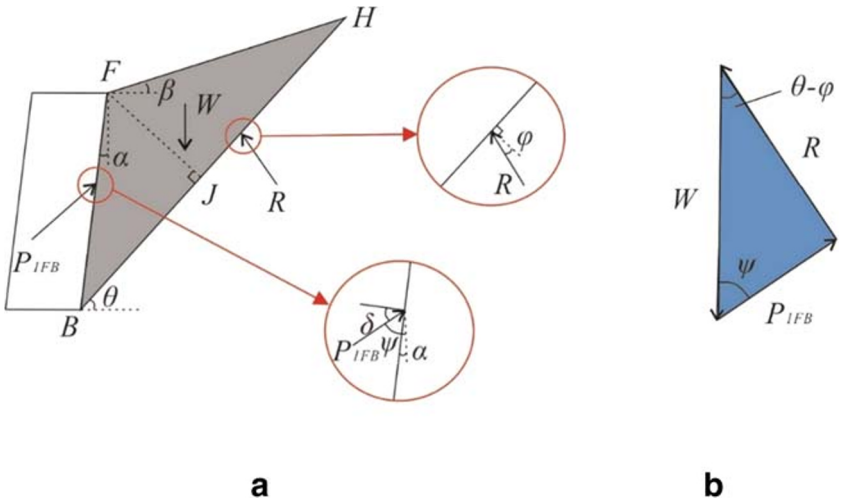

Fig. 5 The soil arching axis is located behind the failure surface. **a** Force diagram of the soil wedge behind the retaining wall. **b** Triangle of force vectors

retaining wall to the vertical and the angle between the slope surface with the horizontal.

The reaction force of retaining wall to the wedge HFB is active earth pressure, and it is denoted by P_{1FB}. The wedge HFB is in static equilibrium condition under the action of three forces (W, R, P_{1FB}) and such forces would form a closed triangle of force vectors, as shown in Fig. 5b, where $\psi = 90° + \alpha - \delta$.

To solve P_{1FB}, primarily the expression of W must be found, and according to Fig. 5a, if S denotes the area symbol, γ is the bulk unit weight of retained soil and h_o is the height of retaining wall, then W will be given by

$$W = S_{HFB} \cdot \gamma \tag{4}$$

where S_{HFB} can be expressed as

$$\begin{aligned} S_{HFB} &= \frac{BH \cdot FJ}{2} = \frac{1}{2} \cdot \left[\frac{h_0}{cos\alpha} \cdot \frac{sin(\alpha + \beta + 90°)}{sin(\theta - \beta)} \right] \\ &\quad \cdot \left[h_0 \cdot \frac{cos(\alpha + \theta)}{cos\alpha} \right] \\ &= \frac{{h_0}^2}{2} \cdot \frac{sin(\alpha + \beta + 90°)cos(\alpha + \theta)}{sin(\theta - \beta)cos^2\alpha} \end{aligned} \tag{5}$$

From the triangle of forces in Fig. 5b, we find

$$\frac{P_{1FB}}{W} = \frac{sin(\theta - \varphi)}{sin(\theta - \varphi + \psi)} \tag{6}$$

Then, P_{1FB} can be figured out as

$$P_{1FB} = W \cdot \frac{sin(\theta - \varphi)}{sin(\theta - \varphi + \psi)} \tag{7}$$

The maximum value of P_{1FB} is found by making

$$\frac{dP_{1FB}}{d\theta} = 0 \tag{8}$$

It is possible to find the angle θ so that the value of P_{1FB} is the maximum.

Thus, the load against retaining wall F could be obtained by comparing the value of E_{1FI} and P_{1FB}.

The soil arch axis located in front of the top of the active failure surface

When the soil arching axis is before the top of the failure surface, the residual sliding force E_{2FI} derived from the soil mass OFIO' could be calculated by adopting the transfer coefficient method.

For solving the active earth pressure P_{2FB} produced by the wedge OFBE, the force analysis of the wedge should be carried out first, as shown in Fig. 6.

The reaction force of retaining wall to the wedge OFBE is active earth pressure, and it is denoted by P_{2FB}. The wedge OFBE is in static limit equilibrium condition under the action of three forces (W, R, P_{2FB}) and such forces would form a closed triangle of force vectors, as shown in Fig. 6b, where $\psi = 90° + \alpha - \delta$.

To solve P_{2FB}, primarily the expression of W must be found, and according to Fig. 6a, if S denotes the area symbol, γ is the bulk unit weight of the retained soil and h_o is the height of retaining wall, then W will be given by

$$W = S_{OFBE} \cdot \gamma \tag{9}$$

According to Fig. 4b, where S_{OFBE} can be expressed as

$$\begin{aligned} S_{OFBE} &= S_{FDEO} + S_{FBC} - S_{BCD} \\ &= \frac{h}{2}(h_0 - h_0 tan\alpha tan\theta + h_0 - htan\theta - h_0 h_0 tan\alpha tan\theta) \\ &\quad + \frac{h_0^2}{2} tan\alpha - \frac{h_0^2}{2} tan^2\alpha tan\theta \\ &= h_0 \left(h + \frac{h_0}{2} tan\alpha \right)(1 - tan\alpha tan\theta) \\ &\quad + \frac{h_0^2}{2}(tan\beta - tan\theta) \end{aligned} \tag{10}$$

From the triangle of forces in Fig. 6b, we find

$$\frac{P_{2FB}}{W} = \frac{sin(\theta - \varphi)}{sin(\theta - \varphi + \psi)} \tag{11}$$

Then, P_{2FB} can be figured out as

$$P_{2FB} = W \cdot \frac{sin(\theta - \varphi)}{sin(\theta - \varphi + \psi)} \tag{12}$$

The maximum value of P_{2FB} is found by making

$$\frac{dP_{2FB}}{d\theta} = 0 \tag{13}$$

It is possible to find the angle θ so that the value of P_{2FB} is the maximum.

Consequently, the load against retaining wall F could be obtained by comparing the value of E_{2FI} and P_{2FB}.

Case study

Project background

The example slope is located on the right side of section DK70 + 432.83 to DK70 + 334, 44.76 m in length, along the railway from Baiyi District in Bazhong City to Shiqiao

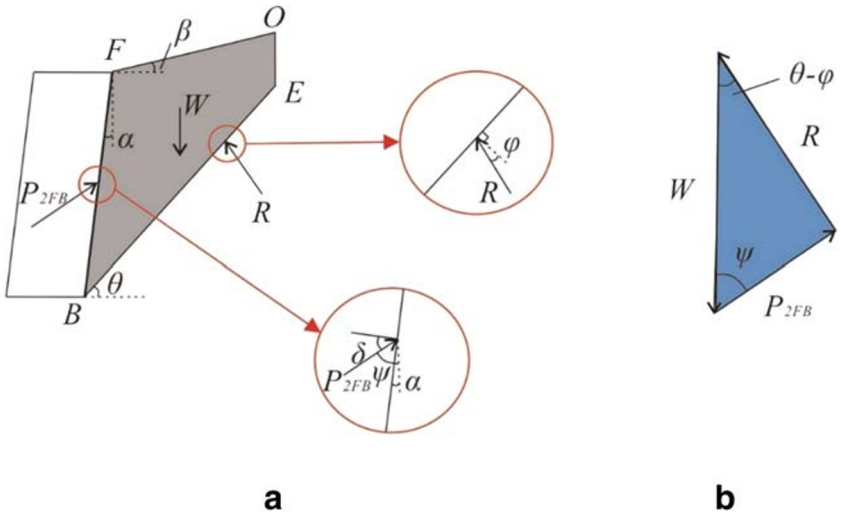

Fig. 6 The soil arching axis is located before the failure surface. **a** Force diagram of the soil wedge behind the retaining wall. **b** Triangle of force vectors

District in Dazhou City, China (see Fig. 7). The slope is composed of mudstone of the Upper Jurassic Penglai formation (J_{3p}), and is divided into three layers along the depth, as shown in Fig. 8a (residual soil, strong-weathered bedrock, and weak-weathered bedrock).

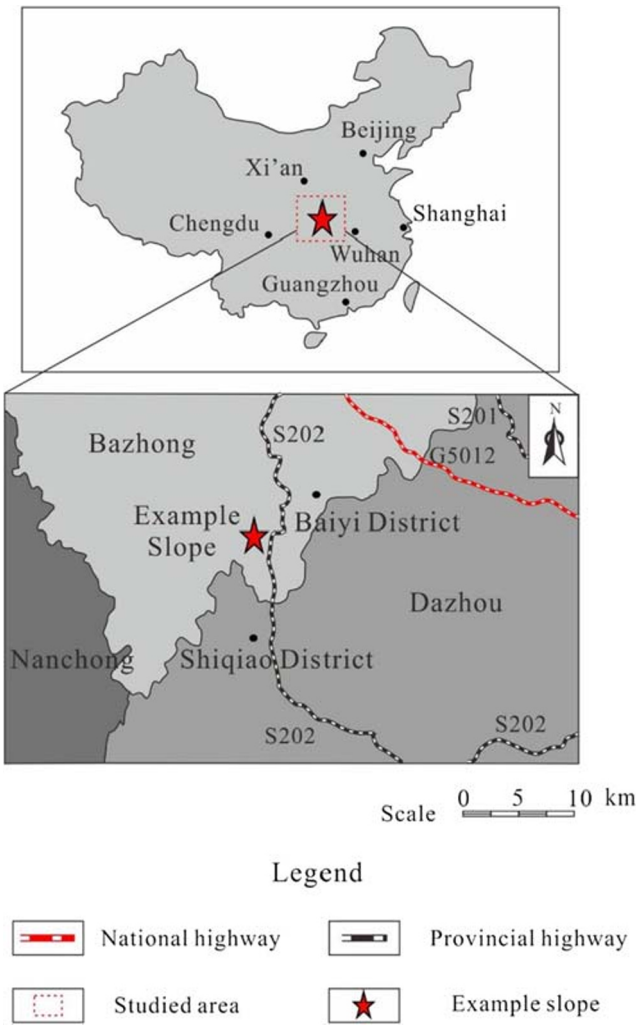

Fig. 7 Location of the example slope

The determination of potential failure surface

The sliding surface of the slope was found based on the arc sliding method, and the result is shown in Fig. 8a. In order to stabilize the slope, a composite retaining structure of stabilizing piles combined with retaining wall was used, as shown in Fig. 8b. The stabilizing piles were installed at the toe of the slope, and the retaining wall was built between the piles.

In this application example, the cross-section dimensions of stabilizing pile are 2 × 2.5 m (width × height) with a center-to-center distance of 6 m. From Eq. (1), the height of soil arch axis is 3 m. Then, the unstable soil mass is divided into slices by vertical planes, and the soil arch axis is represented by the dashed line, as shown in Fig. 8b. The physical and mechanical parameters of the soil mass are shown in Table 1.

Load calculation

Load on stabilizing piles without considering the soil arch effect

In this example, the Railway Design Code of retaining structures of railway embankment (Standardization Administration of China 2006) is used to select the design factor for safety. Thus, based on the code mentioned above, a factor of safety of $k_0 = 1.2$ is obtained. As shown in Fig. 8b, the example slope is divided into slices. For calculating the residual sliding force, use the transfer coefficient method when the soil arching effect is not considered. Therefore, the residual sliding force on stabilizing piles should be the residual sliding force of the 11th slice, and the results are shown in Table 2, where the residual sliding force is 297.4 kN/m.

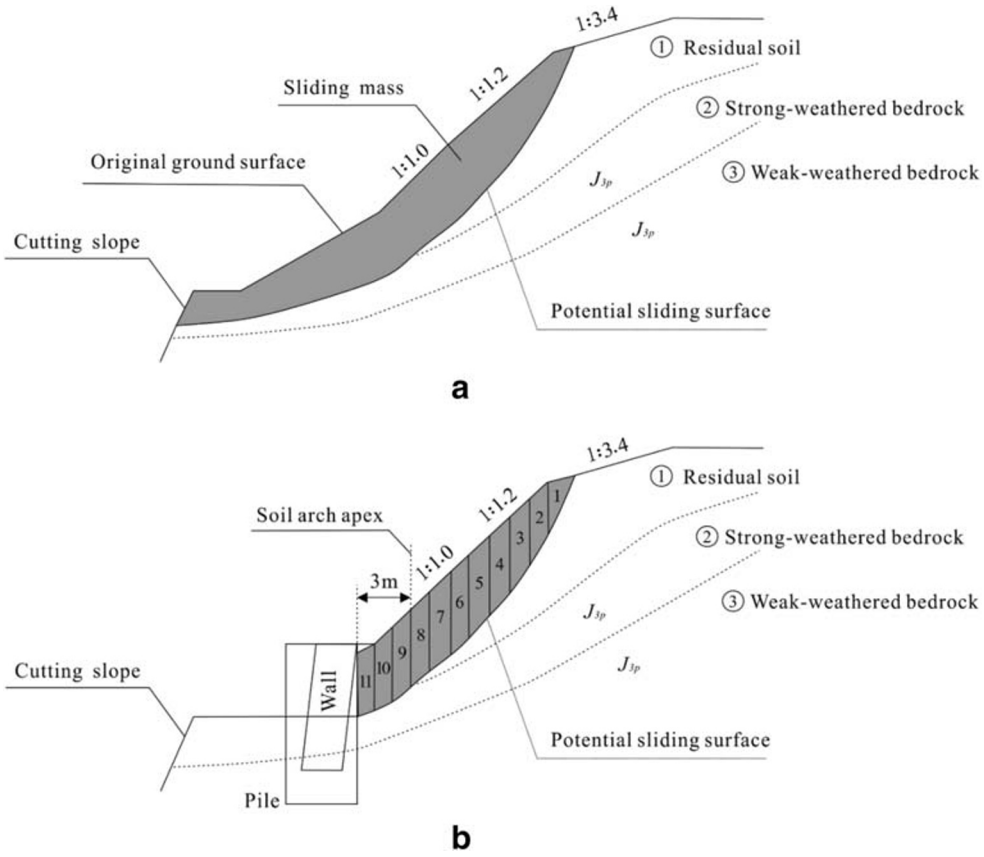

Fig. 8 Profile of the example slope. **a** Initial slope. **b** Slope reinforced with stabilizing piles and retaining wall

Load on stabilizing pile based on the soil arch effect

When the soil arch effect is considered, the load on stabilizing piles is the residual sliding force derived from rear soil mass. As shown in Fig. 8b, the load on the pile should be the residual sliding force transferred by the 8th slice to the soil arch axis. From Table 2, the residual sliding force at the bottom of the 8th slice is 306.1 kN/m.

Load on retaining wall without considering the soil arch effect

The method on the calculation of active earth pressure acting on the retaining wall is proposed based on Coulomb theory which assumes that the retained soil is granular and its cohesion (c) equals 0. Thus, the soil failure criterion is not governed by the friction angle (φ) and cohesion (c) together, but by the friction angle (φ) only.

However, in actual cases, the soil is usually a mixed cohesive-frictional material, rather than granular material. In order to consider the influence of cohesion (c) on active earth pressure, the equivalent internal friction angle φ_D based on the principle of equal shear strength is adopted.

The shear strength of mixed cohesive-frictional material can be described as

$$\tau_f = c + \sigma tan\varphi \tag{14}$$

According to the principle of equal shear strength, the shear strength of equivalent granular material can be expressed as

$$\tau_f = \sigma tan\varphi_D \tag{15}$$

Consequently, the equivalent internal friction angle φ_D can be written as

$$\varphi_D = \arctan\left(tan\varphi + \frac{c}{\sigma}\right) = \arctan\left(tan\varphi + \frac{c}{\gamma h_0}\right) \tag{16}$$

Where c and φ are the shear strength parameters of mixed cohesive-frictional material; γ is the bulk unit weight of the material and h_0 is the retaining wall height.

In this application example, the angle between the back of the retaining wall and the vertical is 15°. As mentioned above,

Table 1 Physical and mechanical parameters of the soil constituting the example slope

Rock or soil layer	Bulk unit weight r (kN/m^3)	Cohesion c (kPa)	Friction angle φ (°)
①	18.5	12	30
②	23	/	40

Table 2 Calculation of the residual sliding force

Slice no.	Slice weight W_i (kN/m)	Slice width L_i (m)	Slip surface angle α_i (°)	Transfer coefficient Ψ_i	Slice force T_i (kN/m)	Anti-slide force R_i (kN/m)	Residual sliding force E_i (kN/m)
1	50.1	1.7	64	0.0000	54.0	33.6	20.5
2	104.3	1.5	59	0.9459	107.3	49.0	77.6
3	130.3	1.5	54	0.9459	126.5	62.2	137.7
4	148.4	1.5	50	0.9573	136.4	73.1	195.1
5	159.6	1.5	46	0.9573	137.7	82.0	242.6
6	138.0	1.3	43	0.9684	113.0	73.9	274.0
7	147.4	1.4	40	0.9684	113.7	82.0	297.0
8	130.3	1.3	37	0.9684	94.1	75.7	306.1
9	94.5	1.0	35	0.9792	65.0	56.7	308.0
10	88.3	1.0	33	0.9792	57.7	54.7	304.6
11	90.6	1.0	31	0.9792	56.0	56.8	297.4

Notes: $T_i = W_i k_o \sin\alpha_i$, $R_i = W_i k_o \sin\alpha_i \tan\varphi_i + C_i L_i$, $E_i = \psi_i E_{i-1} + T_i - R_i$, $\psi_i = \cos(\alpha_{i-1} - \alpha_i) - \sin(\alpha_{i-1} - \alpha_i)\tan\varphi_i + 1$

the height of soil arch axis is 3 m. According to Eqs. (9)~(13) and (16), the equivalent internal friction φ_D, the friction angle between the back of retaining wall and the retained soil δ, the angle between the active failure surface and the horizontal θ could be obtained with 34°, 15°, 44°, respectively.

When the soil arching effect is not considered, the load on retaining wall should be active earth pressure produced by the wedge BEDF, as shown in Fig. 9a. Based on the Coulomb theory, the active earth pressure produced by the wedge is obtained and equals 69.0 kN/m.

Load on retaining wall based on the soil arch effect

Considering the soil arch effect, the load on the retaining wall should be the maximum between active earth pressure produced by the wedge AEDFC and residual sliding force derived from front soil mass, as shown in Fig. 9b. According to the formulas (9) to (13), the active earth pressure equals 53.7 kN/m. The residual sliding force acting on the wall should be the residual sliding force generated by slices 9, 10, 11, and the results are shown in Table 3. According to Table 3, we can know the residual sliding force is only 10.0 kN/m. Hence, the load on the retaining wall should adopt active earth pressure.

Analysis of results

The results of the above calculation are summarized in Table 4. This table shows that the soil arching effect does affect the load distribution between the stabilizing piles and retaining wall. Especially, the load on the retaining wall is greatly affected by the soil arch, and the difference reaches a rate of 22.2%.

In Table 4, there is no significant difference between the load against the stabilizing pile considering the soil arching effect and without considering the soil arching effect because there is no obvious anti-slide part, that is, the dip angle of the last few slices is still large. However, when there is a clear anti-slide part, the load on stabilizing piles would increase obviously due to the soil arch, as shown in Fig. 10a. Of course, when there is a clear slide part, the load on stabilizing piles would decrease accordingly subjected to the effect of soil arch, as shown in Fig. 10b.

Discussions

The impact of assuming the height of soil arch to be same along the vertical direction

The novel soil arch model was proposed based on an assumption that the height of soil arch is constant along the vertical direction, while the height of soil arch keeps decreasing gradually in practice, since the soil arching effect should progressively vanish in the proximity of the ground level, as shown in Fig. 11. Owing to neglecting the difference of height of soil arch at various depths, the scope of front and rear soil mass would change from OFGO″, KOO” to OFGO’, KOO’, respectively. Consequently, the theoretical load against the retaining wall is higher than the actual value as the scope of front soil mass increases, leading to that the design of retaining wall tends to be conservative. For the load on stabilizing piles, due to the scope of rear soil mass decreasing, the theoretical value is less than the actual one. However, considering that the reduced range of rear soil mass (OO’O”) is much smaller than the theoretical scope (KOO’), the difference between the theoretical load on stabilizing pile and the actual value would be

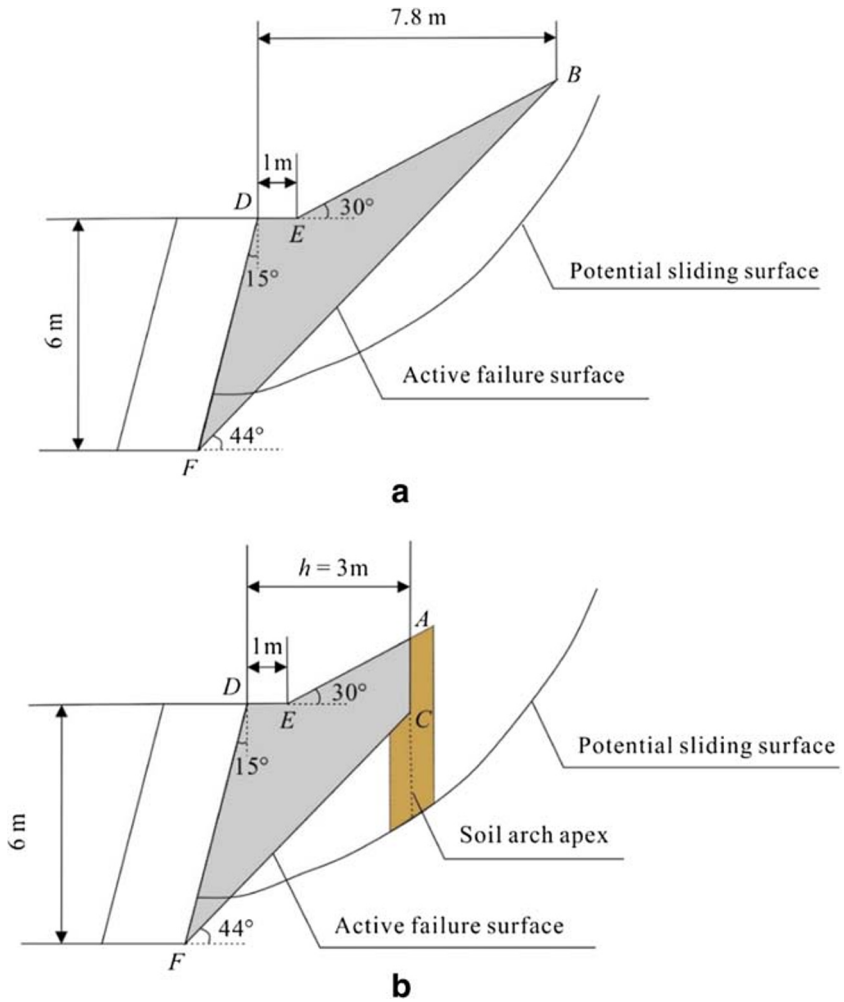

Fig. 9 Range of the sliding wedge. **a** Without considering the soil arch effect. **b** Considering the soil arch effect

extremely small, thus the theoretical one is rational for engineering design. In summary, the effects of neglecting the height change of soil arch on the design of stabilizing piles and retaining wall are acceptable in practice despite the inaccurate assumption.

Consideration on the optimization of the inclination angle of soil arch model

In slope engineering practices, the retained soil with different properties tends to form an arch with a different inclination angle (Guo and Zhou 2013; Rui et al. 2016). Such as the finding by Quinlan and Lobban (Quinlan 1987) that granular soils would form a tall arch, whereas cohesive deposits favor the development of a flat arch, since the inclination angle of soil arch mainly depends on the friction angle of soil. The soil arch model presented in this paper directly stipulates that the inclination angle α of the soil arch is 45^c, without considering the influence of the friction angle of soil, probably leading to an inaccurate design. In future research, the soil arch model with different inclination angle α will be separately proposed in detail based on the retained soil with different friction angle (Fig. 12).

Table 3 Calculation of residual sliding force on the retaining wall considering the soil arch effect

Slice no.	Slice weight W_i (kN/m)	Slice width L_i (m)	Slip surface angle α_i (°)	Transfer coefficient Ψ_i	Slice force T_i (kN/m)	Anti-slide force R_i (kN/m)	Residual sliding force E_i (kN/m)
9	94.5	1.0	35	0	65.0	56.7	8.3
10	88.3	1.0	33	0.9792	57.7	54.7	11.1
11	90.6	1.0	31	0.9792	56.0	56.8	10.0

Table 4 Calculation results of the example slope

Load type	No soil arch effect F_1/(kN/m)	With soil arch effect F_2/(kN/m)	Difference rate $\frac{\lvert F_2-F_1\rvert}{F_1}$/%
On pile	297.4	306.1	2.9
On the retaining wall	69.0	53.7	22.2

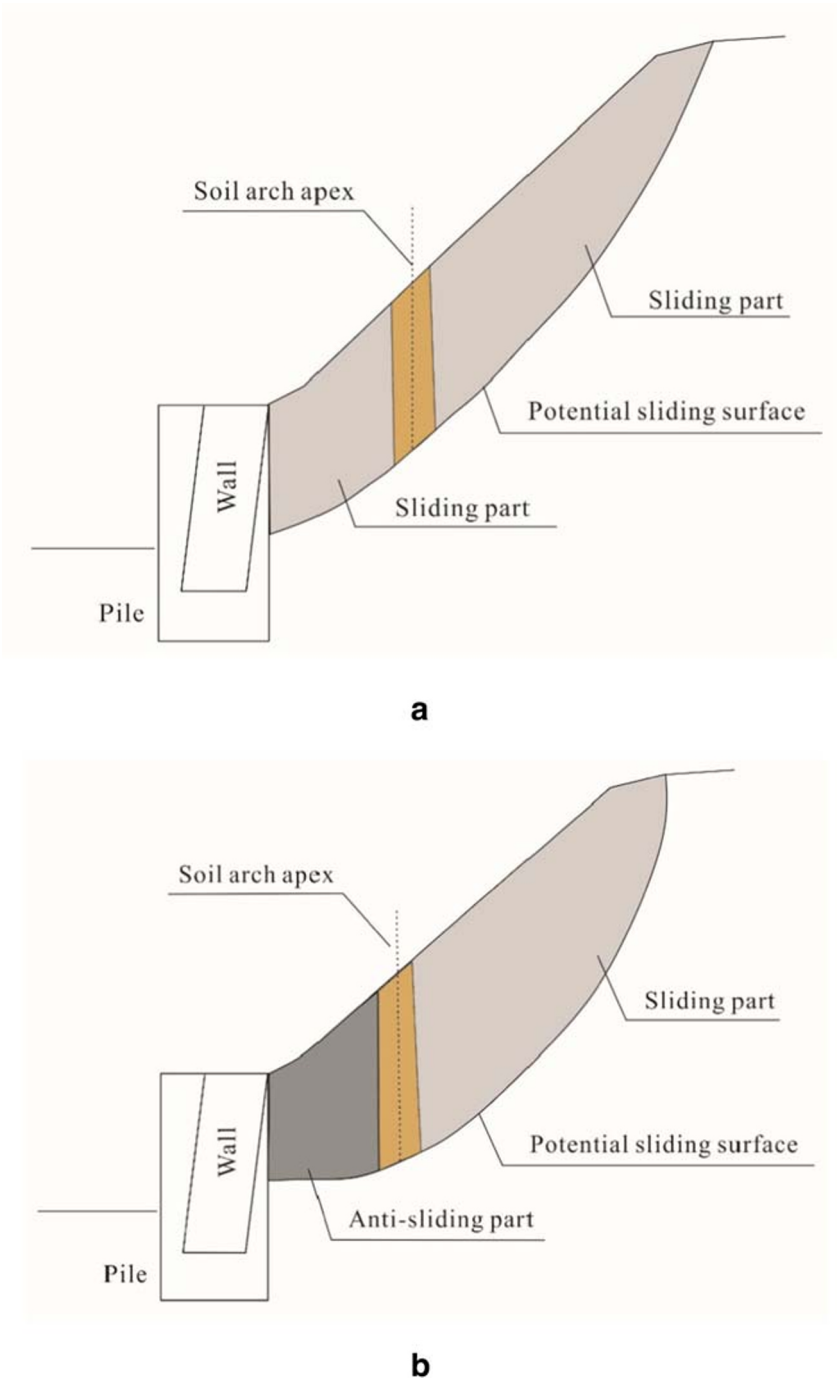

Fig. 10 Sketches for potential sliding surface. **a** With anti-sliding part. **b** Without anti-sliding part

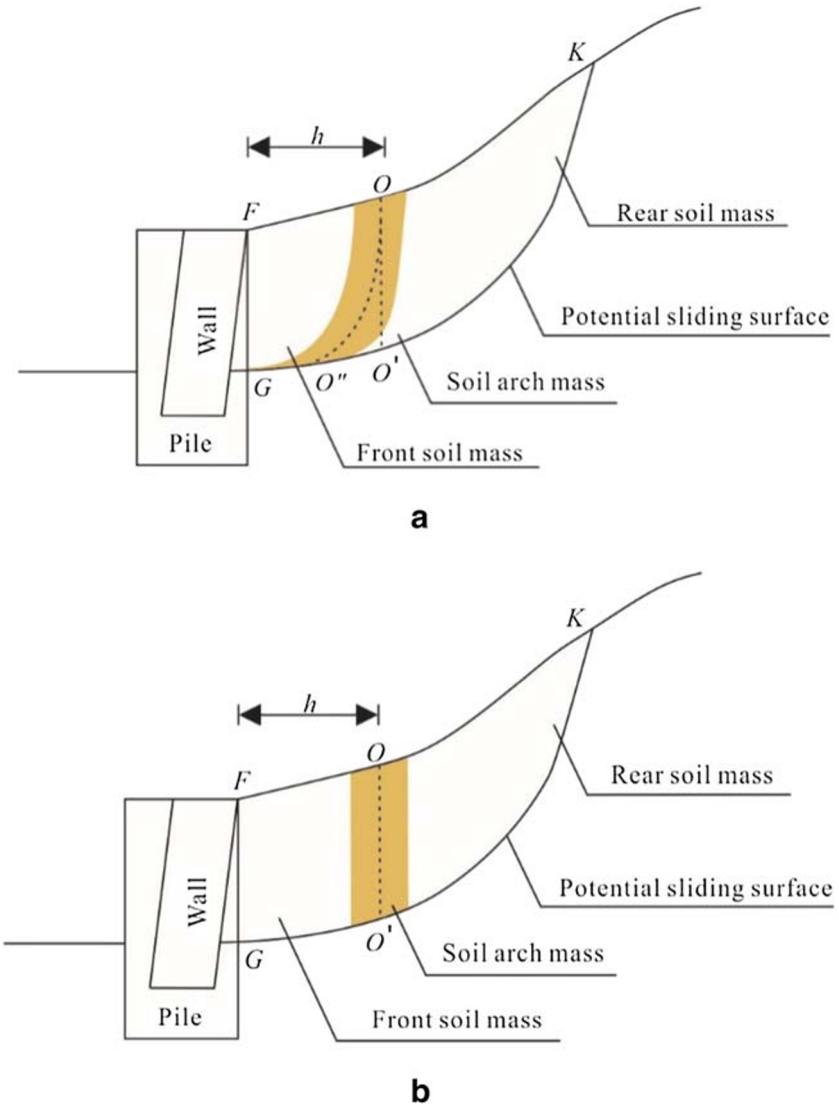

Fig. 11 Height change of soil arch along the vertical direction. **a** Decreasing in practice. **b** unchanging in this paper

Comparison between the traditional method and the simplified method

Although many researchers have contributed a great deal to the design of composite retaining structures (Lin et al. 2018; Wang et al. 2014), they have seldom accurately evaluated the load distribution between stabilizing piles and retaining wall due to that the soil arching effect was ignored or unreasonably considered. Traditionally, residual sliding force derived from whole unstable soil was used as the load on stabilizing piles, and load against retaining wall commonly adopted the active earth pressure or its reduction value. Such a method was largely inaccurate and caused unreasonable design.

In order to rationally consider soil arch effect, the simplified method theoretically defines the scope of front and rear soil mass based on an ideal soil arch model, then considers that the load on stabilizing piles and retaining wall are attributed to front and rear soil mass respectively. In light of that the failure mode of rear soil mass is sliding failure and the failure mode of front soil mass is collapsing or sliding failure, the residual sliding force derived from rear soil mass is used as the ultimate load against stabilizing piles, and the ultimate load on retaining wall adopts the active earth pressure originated from the sliding wedge before arch or the residual sliding force produced by front soil mass.

However, not all cut slope designs have to consider soil arching effect. If the internal frictional angle φ of slope material is almost 0 in cohesive (c) soil slope design, the simplified and traditional methods would show similar results since the soil arching effect is not obvious. Similarly, soil arching also seldom occurs obviously in frictional (φ) soil slope or cohesive-frictional (c-φ) soil slope where the internal frictional angle φ of slope material is small. For a quick analysis, we tentatively propose empirical suggestions about the soil arching effect can be ignored rationally in what situation: (1) the internal frictional angle φ of slope material is less than 5°

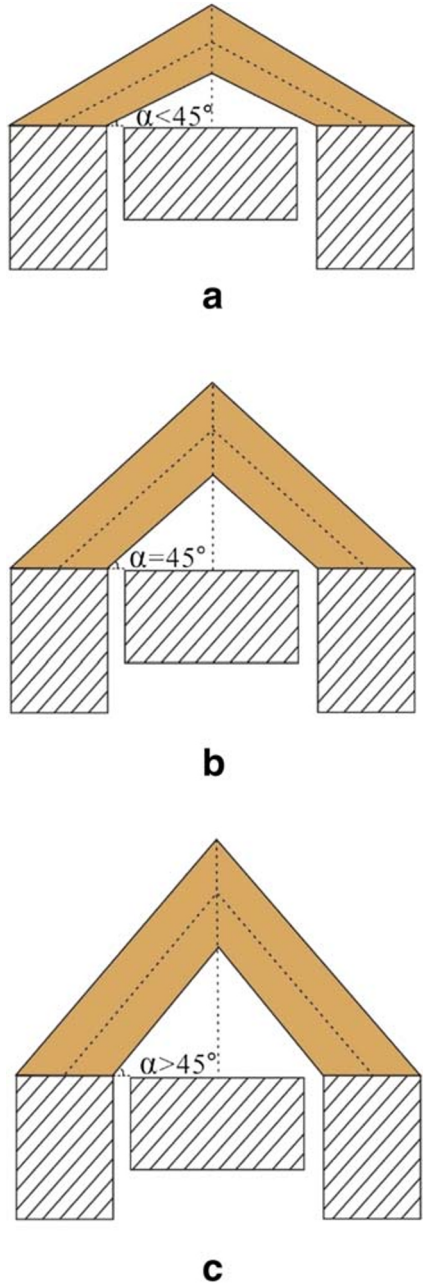

Fig. 12 Soil arch model with different inclination angle α. **a** α < 45°. **b** α = 45°. **c** α > 45°

in cohesive (c) soil slope design; (2) the internal frictional angle φ of slope material is less than 10° in frictional (φ) soil slope or cohesive-frictional (c-φ) soil slope design.

In this paper, we took a cutting slope on the Bazhong-Dazhou Railway as an example to discuss the composite retaining structures design difference between traditional method ignoring soil arching effect and simplified method based on soil arching effect. The results highlight that whether soil arching effect is considered or not, the difference of load against stabilizing piles is merely 2.9%. This is mainly due to that there is no obvious anti-slide part in this case study. However, the load on the retaining wall would be greatly affected by soil arching. Through adopting the simplified method based on the soil arching effect, the load on retaining wall is 22.2% lower than that calculated by the traditional method ignoring soil arching effect. Compared with the traditional method, the simplified method could analytically calculate the load distribution between stabilizing piles and retaining wall, providing a more reasonable design for both safety and economical purposes.

Conclusions

In order to design composite retaining structures better and avoid unnecessary investments, a novel soil arch model was proposed with the characteristics of three-dimensional soil arch mass. Such soil arch separates retained soil into three parts: soil arch mass, front soil mass, and rear soil mass. On the basis, soil arch effect on the load distribution between stabilizing piles and retaining wall was analyzed theoretically. The residual driving force derived from rear soil mass was used as the load on stabilizing piles, and the load against retaining wall adopted the active earth pressure originated from the sliding wedge before arch or the residual sliding force produced by front soil mass. Then, a simplified method for calculating the load on stabilizing piles and retaining wall respectively was put forward, by considering the soil arch effect in different situations, including when the soil arch axis was located before and after the top of active failure surface.

A cutting slope reinforced by the stabilizing piles combined with retaining wall on the Bazhong-Dazhou Railway is carried out as an application example. When the soil arch effect is considered, the simplified method mentioned in this paper is adopted to calculate the load on stabilizing piles and retaining wall, respectively, and the result is obviously different from another obtained by the conventional method where the soil arch effect is ignored. In particular, the load on the retaining wall decreases dramatically, by 22.2%, which would greatly influence the design of retaining wall between the piles.

To carry out the evaluation of soil arch effect on the load distribution between the composite retaining structures more simple, this paper assumes that the height of soil arch is constant along the vertical direction and inclination angle of soil arch is not affected by the friction angle of the retained soil. Although the influence of such assumptions on the design of the composite retaining structure is not very seriously and acceptable in practice, it still deserves to be studied further.

Acknowledgments The work was funded by the National Natural Science Foundation of China (no. 41672295) and the Science and Technology Project of Department of Transportation of Sichuan Province (no. 2015B1-1). The authors would like to extend their most sincere gratitude to the Editors and Reviewers who provided help during the writing of this paper.

References

Ahmadi A, Seyedi Hosseininia E (2018) An experimental investigation on stable arch formation in cohesionless granular materials using developed trapdoor test. Powder Technol 330:137–146

Alejano LR, Gómez-Márquez I, Martínez-Alegría R (2010) Analysis of a complex toppling-circular slope failure. Eng Geol 114(1–2):93–104

Aydin A, Ozbek A, Cobanoglu I (2004) Tunnelling in difficult ground: a case study from Dranaz tunnel, Sinop, Turkey. Eng Geol 74(3–4): 293–301

Bi R, Ehret D, Xiang W et al (2012) Landslide reliability analysis based on transfer coefficient method: a case study from three gorges reservoir. J Earth Sci 23(2):187–198

Chen CY, Martin GR (2002) Soil–structure interaction for landslide stabilizing piles. Comput Geotech 29(5):363–386

Chevalier B, Combe G, Villard P (2007) Load transfers and arching effects in granular soil layer. 18eme Congres Franrais de Mecanique Grenoble aout, pp: 27–31

Ehrlich M, Silva RC (2015) Behavior of a 31m high excavation supported by anchoring and nailing in residual soil of gneiss. Eng Geol 191: 48–60

Ersöz T, Topal T (2018) Weathering and excavation effects on the stability of various cut slopes in Flysch-like deposits. Geotech Geol Eng 36(6):3707–3729

Galli A, di Prisco C (2013) Displacement-based design procedure for slope-stabilizing piles. Can Geotech J 50(1):41–53

Goel S, Patra NR (2008) Effect of arching on active earth pressure for rigid retaining walls considering translation mode. Int J Geomech 8(2):123–133

Guo P, Zhou S (2013) Arch in granular materials as a free surface problem. Int J Numer Anal Met 37(9):1048–1065

Handy RL (1985) The arch in soil arching. J Geotech Eng 111(3):302–318

Harrop-williams KO (1987) Geostatis wall pressures. J Geotech Eng ASAE 113(3):273–276

Hu J, Ma F (2018) Failure investigation at a collapsed deep open cut slope excavation in soft clay. Geotech Geol Eng 36(1):665–683

Iglesia GR, Einstein HH, Whitman RV (2014) Investigation of soil arching with centrifuge tests. J Geotech Geoenviron Eng 140(2): 1–13

Ito T, Matsui T (1975) Methods to estimate lateral force acting on stabilizing piles. Soils Found 21:21–37

Jiang C, Zhao X, Li Q et al (2010) Discussion on design theory on joint use of pile and soil-nailing or retaining walls. J Rai Eng Soc 4(139): 35–39 (in Chinese)

Khatami H, Deng A, Jaksa M (2019) An experimental study of the active arching effect in soil using the digital image correlation technique. Comput Geotech 108:183–196

Kingsley HW (1989) Arch in soil arching. J Geotech Eng ASCE 115(3): 415–419

Krabbenhoft K (2019) Plastic design of embedded retaining walls. P I Civil Eng-Geotec 172(2):131–144

Lai H, Zheng J, Zhang R et al (2018) Classification and characteristics of soil arching structures in pile-supported embankments. Comput Geotech 98:153–171

Li C, Wu J, Tang H et al (2015) A novel optimal plane arrangement of stabilizing piles based on soil arching effect and stability limit for 3D colluvial landslides. Eng Geol 195:236–247

Li C, Yan J, Wu J et al (2019) Determination of the embedded length of stabilizing piles in colluvial landslides with upper hard and lower weak bedrock based on the deformation control principle. Bull Eng Geol Environ 78(2):1189–1208

Liang Y, Jiang C, Li Q et al (2014) Analysis of stress mechanism of pile composite structure based on soil arch test. Chin J Rock Mech Eng 33(s2):3825–3828 (in Chinese)

Lin P, Lim A, Ho S et al (2018) Application of the novel composite earth retaining structure method to urban excavations: a constructability analysis. J Chin Inst Eng 41(7):603–611

Lirer S (2012) Landslide stabilizing piles: experimental evidences and numerical interpretation. Eng Geol 149-150:70–77

Martin CD, Bartz JR, Hendry MT (2019) Design procedure for landslide stabilization using sheet pile ribs. Can Geotech J 56(4):514–525

McKelvey JA III (1994) The anatomy of soil arching. Geotext Geomembr 13:317–329

Mohammadi S, Taiebat H (2016) Finite element simulation of an excavation-triggered landslide using large deformation theory. Eng Geol 205:62–72

Pain A, Choudhury D, Bhattacharyya SK (2017) Seismic passive earth resistance using modified pseudo-dynamic method. Earthq Eng Eng Vib 16(2):263–274

Pirone M, Urciuoli G (2018) Analysis of slope-stabilising piles with the shear strength reduction technique. Comput Geotech 102:238–251

Qin CB, Chian SC, Wang CY (2017) Kinematic analysis of pile behavior for improvement of slope stability in fractured and saturated Hoek-Brown rock masses. Int J Numer Anal Met 41(6):803–827

Quinlan JF (1987) Discussion of "the arch in soil arching" by R. L Handy. J Geotech Geoenviron 113(3):272–274

Rincon O, Shakoor A, Ocampo M (2016) Investigating the reliability of H/V spectral ratio and image entropy for quantifying the degree of disintegration of weak rocks. Eng Geol 207:115–128

Rui R, van Tol F, Xia X et al (2016) Evolution of soil arching; 2D DEM simulations. Comput Geotech 73:199–209

Standardization Administration of China (2006) TB 10026-2006: code for design on retaining structures of railway embankment. Standardization Administration of China, Beijing (in Chinese)

Standardization Administration of Chongqing, China (2004) DB50/5029-2004: code for design on geological hazard prevention engineering. Urban And Rural Construction Committee, Chongqing (in Chinese)

Terzaghi K (1943) Theoretical soil mechanics. Wiley, New York, pp 76–85

Vardoulakis L, Graf B, Gudehus G et al (1981) Trap-door problem with dry sand: a statical approach based upon model test kinematics. Int J Numer Anal Met 5(1):57–78

Vrecl Kojc H, Trauner L (2010) Upper-bound approach for analysis of cantilever retaining walls. Can Geotech J 47(9):999–1010

Wang J, Liang Y, Zhang H et al (2014) A loess landslide induced by excavation and rainfall. Landslides 11(1):141–152

Wu J, Li C, Liu Q et al (2017) Optimal isosceles trapezoid cross section of laterally loaded piles based on friction soil arching. KSCE J Civ Eng 21(7):2655–2664

Xiao S, Zeng J, Yan Y (2017) A rational layout of double-row stabilizing piles for large-scale landslide control. Bull Eng Geol Environ 76(1): 309–321

Yilmazer I, Yilmazer O, Saraç C (2003) Case history of controlling a major landslide at Karandu, Turkey. Eng Geol 70(1–2):47–53

Zhang Y, Hu X, Tannant DD et al (2018) Field monitoring and deformation characteristics of a landslide with piles in the three gorges reservoir area. Landslides 15(3):581–592

Zhang Z, Wang T, Wu S et al (2017) The role of seismic triggering in a deep-seated mudstone landslide, China: historical reconstruction and mechanism analysis. Eng Geol 226:122–135

Zheng Y, Chen C, Liu T et al (2015) Analysis of toppling failure of rock slopes under the loads applied on the top. Rock Soil Mech 36(9): 2639–2647 +2658 (in Chinese)

Zhou Y, Chen Q, Chen F et al (2018) Active earth pressure on translating rigid retaining structures considering soil arching effect. Eur J Environ Civ Eng 22(8):910–926